Examination of the surrogate ratio method for the determination of the ^{93}Zr$(n,\gamma)^{94}$Zr cross section with ^{90,92}Zr$(^{18}$O$,^{16}$O$)^{92,94}$Zr reactions

S. Q. Yan (颜胜权),[1,*] Z. H. Li (李志宏),[1] Y. B. Wang (王友宝),[1] K. Nishio,[2] H. Makii,[2] J. Su (苏俊),[1] Y. J. Li (李云居),[1] I. Nishinaka,[2] K. Hirose,[2] Y. L. Han (韩银录),[1] R. Orlandi,[2] Y. P. Shen (谌阳平),[1] B. Guo (郭冰),[1] S. Zeng (曾晟),[1] G. Lian (连钢),[1] Y. S. Chen (陈永寿),[1] X. X. Bai (白希祥),[1] L. H. Qiao (乔律华),[1] and W. P. Liu (柳卫平)[1]

[1]*China Institute of Atomic Energy, P.O. Box 275(10), Beijing 102413, People's Republic of China*

[2]*Japan Atomic Energy Agency, Tokai, Naka, Ibaraki 319-1195, Japan*

(Received 29 January 2016; published 14 July 2016)

The relative γ-decay probability ratios of the neutron resonance states in ^{94}Zr and ^{92}Zr populated via two-neutron transfer reactions, ^{92}Zr$(^{18}$O$,^{16}$O$)^{94}$Zr and ^{90}Zr$(^{18}$O$,^{16}$O$)^{92}$Zr, have been measured to test the validity of the surrogate ratio method (SRM) in determining the (n,γ) reaction cross section. The cross sections of the ^{93}Zr$(n,\gamma)^{94}$Zr reaction are derived from the experimentally obtained ratios and the cross sections of the ^{91}Zr$(n,\gamma)^{92}$Zr reaction in the equivalent neutron energy range of $E_n = 0$–8 MeV. The deduced cross sections of ^{93}Zr$(n,\gamma)^{94}$Zr reaction agree with the directly measured ones in the low-energy region, and with the evaluated ENDF/B-VII.1 data at higher energies of $E_n > 3$ MeV. The agreement supports the concept of the SRM method to indirectly determine the (n,γ) reaction cross sections.

DOI: 10.1103/PhysRevC.94.015804

I. INTRODUCTION

Whether for nuclear reactors on the earth or massive stars in the universe, there are many radionuclides mixed in their fuels, and neutron radiative capture reactions of such radionuclides play an important role in the energy generation and nucleosynthesis [1–5]. Up to date, the cosmic origin of elements heavier than iron is believed to be of slow and rapid neutron capture processes, and a large number of (n,γ) reactions of radionuclides are intensely involved in the relevant reaction networks. However, the (n,γ) cross sections are hard to measure directly because of the difficulty of preparing target materials of the short-lived radionuclides. Instead, several indirect methods have been proposed, and many experimental investigations have been carried out. The surrogate method (SM) [6–10], first introduced in the 1970s for the extraction of neutron-induced fission cross sections [11], was recently used to determine the (n,γ) reaction cross sections. Based on the Weisskopf-Ewing limit of the Hauser-Feshbach theory [12] which assumes that the decay probability of a compound nucleus (CN) is independent from its spin parity, the method makes use of a surrogate reaction with available beam and target to produce the same CN as the neutron capture process. The cross section of the (n,γ) reaction is then indirectly determined by calculated the CN formation cross section multiplying the measured γ-decay probability.

The surrogate ratio method (SRM) is a variation of the surrogate method. In this method, two surrogate reactions are employed to obtain the relative γ-decay probability ratio. With an available (n,γ) reaction cross section as the reference, the aimed (n,γ) reaction cross section can be obtained by multiplying the reference reaction cross section to the ratio measured experimentally with the SRM. The SRM was successfully applied in the (n,f) cross section determination [13–19], and a comprehensive review was recently given by Escher *et al.* [20]. In the case of (n,γ) reactions, theoretical studies [21–23] indicate that the γ-decay probability is more sensitive to the spin parity of the CN in the low neutron energy region; a large difference was indeed observed recently between the results deduced with SM and the directly measured ones [24–26]. Comparing with SM, the SRM is likely to compensate the difference of the spin distribution between the neutron capture process and the surrogate reaction by taking the ratio of the γ-decay probability.

The recent application of SRM for the (n,γ) reaction was mainly concentrated in inelastic scattering reactions such as (p,p'), $(^3$He$,^3$He$')$, (α,α') [25,27,28], and one-neutron transfer reactions such as (d,p), $(^3$He$,\alpha)$ reactions [24,27,29,30]. To apply the SRM to the (n,γ) reactions of more neutron-rich nuclei, it is important to test the validity of SRM with two or more neutron transfer reactions. In the present work, two-neutron transfer reactions $(^{18}$O$,^{16}$O$)$ are employed to check the SRM for the determination of the (n,γ) reaction cross section. The γ-decay probability ratios have been obtained in a wide equivalent neutron energy range from 0 to 8 MeV. The ^{93}Zr$(n,\gamma)^{94}$Zr reaction cross sections are determined relative to the cross sections of the ^{91}Zr$(n,\gamma)^{92}$Zr reaction together with the deduced γ-decay probability ratios.

II. METHOD

The nonresonant (n,γ) reaction is governed by the electromagnetic interaction, and the resonant (n,γ) reaction operates, however, through the strong interaction that characterizes the formation of the compound nucleus. The resonant (n,γ) cross section can be factorized as a production of the formation cross section of CN and the γ-decay probability of the resonance states of CN. Under the Weisskopf-Ewing assumption, the γ-decay probability is independent of the spin parity of CN, therefore, the cross section of A(n,γ)B can be expressed as

$$\sigma_{A(n,\gamma)B}(E_n) = \sigma^{\mathrm{CN}}_{n+A}(E_n) \times G^{\mathrm{CN}}_{B^*\to\gamma+B}(E_n). \quad (1)$$

*Panyu@ciae.ac.cn

In the above equation, $\sigma^{\rm CN}_{n+A}(E_n)$ denotes the CN formation cross section and $G^{\rm CN}_{B^*\to\gamma+B}(E_n)$ represents the γ-decay probability of B*, where E_n is the incident energy of neutron. The CN formation cross section can be determined via an optical model calculation with uncertainties of about 5% [31], while the theoretical γ-decay probabilities have large model dependence and are often quite uncertain. Thus the $G^{\rm CN}_{B^*\to\gamma+B}(E_n)$ needs to be determined experimentally. In the surrogate method, B* is formed via a surrogate reaction: $\mathrm{d}+\mathrm{D}\to\mathrm{b}+\mathrm{B}^*$; the γ decay of CN ($\mathrm{B}^*\to\gamma+\mathrm{B}$) is observed in coincidence with the outgoing particle b. The γ-decay probability can be written as

$$G^{\rm CN}_{B^*\to\gamma+B}(E_{\rm ex})=\frac{N_{B^*\gamma}(E_{\rm ex})}{\epsilon_\gamma N_{B^*}(E_{\rm ex})}. \tag{2}$$

$N_{B^*}(E_{\rm ex})$ is the total number of CN, which can be obtained by counting ejectile nucleus b from the reaction $\mathrm{d}+\mathrm{D}\to\mathrm{b}+\mathrm{B}^*$; $N_{B^*\gamma}(E_{\rm ex})$ is the number of CN that decays into the ground state by emitting γ rays, which also can be directly measured in surrogate method experiment. $E_{\rm ex}$ denotes the excitation energy of CN and ϵ_γ is the efficiency of γ detector. The absolute number of N_{B^*} is needed in the surrogate method, which is usually the source of error because of the difficulty in resolving the contaminant reaction channels.

In the SRM, in addition to the aimed reaction $\mathrm{n}+\mathrm{A1}\to\mathrm{B1}^*\to\gamma+\mathrm{B1}$, another reference reaction $\mathrm{n}+\mathrm{A2}\to\mathrm{B2}^*\to\gamma+\mathrm{B2}$ with known cross section is needed. The ratio of the two reaction cross sections is

$$\begin{aligned}\frac{\sigma_{A1(n,\gamma)B1}(E_n)}{\sigma_{A2(n,\gamma)B2}(E_n)}&=\frac{\sigma^{\rm CN}_{n+A1}(E_n)\times G^{\rm CN}_{B1^*\to\gamma+B1}(E_n)}{\sigma^{\rm CN}_{n+A2}(E_n)\times G^{\rm CN}_{B2^*\to\gamma+B2}(E_n)}\\ &\approx\frac{G^{\rm CN}_{B1^*\to\gamma+B1}(E_n)}{G^{\rm CN}_{B2^*\to\gamma+B2}(E_n)}=\frac{\epsilon_{\gamma2}N_{B1^*\gamma}(E_n)}{\epsilon_{\gamma1}N_{B2^*\gamma}(E_n)}\times\frac{N_{B2^*}(E_n)}{N_{B1^*}(E_n)}.\end{aligned} \tag{3}$$

If the reference reaction is chosen similar to the aimed one, the ratio of the CN formation cross section $\sigma^{\rm CN}_{n+A1}(E_n)/\sigma^{\rm CN}_{n+A2}(E_n)\approx 1$ and the (n,γ) cross section ratio can be simplified to the ratio of γ-decay probabilities.

In the SRM experiment, two surrogate reactions, $\mathrm{d1}+\mathrm{D1}\to\mathrm{b1}+\mathrm{B1}^*$ and $\mathrm{d2}+\mathrm{D2}\to\mathrm{b2}+\mathrm{B2}^*$, are chosen to form the compound nuclei B1* and B2*. The ratio $N_{B2^*}(E_{\rm ex})/N_{B1^*}(E_{\rm ex})$ in Eq. (3) can be determined from the CN formation cross section integrated over the detector solid angle $\sigma^{\rm CN}_{d+D}(E_{\rm ex})$, the thickness of target ρ, the beam current I, and the efficiency of the particle detector ϵ through the relation,

$$\frac{N_{B2^*}(E_{\rm ex})}{N_{B1^*}(E_{\rm ex})}=\frac{\sigma^{\rm CN}_{d2+D2}(E_{\rm ex})}{\sigma^{\rm CN}_{d1+D1}(E_{\rm ex})}\times\frac{\rho_2\times I_2\times\epsilon_2}{\rho_1\times I_1\times\epsilon_1}. \tag{4}$$

If the two surrogate reactions are deliberately chosen to make the $\sigma^{\rm CN}_{d2+D2}(E_{\rm ex})/\sigma^{\rm CN}_{d1+D1}(E_{\rm ex})\approx 1$, Eq. (3) then becomes

$$\begin{aligned}\frac{\sigma_{A1(n,\gamma)B1}(E_n)}{\sigma_{A2(n,\gamma)B2}(E_n)}&\approx\frac{N_{B1^*\gamma}(E_n)}{N_{B2^*\gamma}(E_n)}\times\frac{\epsilon_{\gamma2}\times\rho_2\times I_2\times\epsilon_2}{\epsilon_{\gamma1}\times\rho_1\times I_1\times\epsilon_1}\\ &\approx C_{\rm nor}\frac{N_{B1^*\gamma}(E_n)}{N_{B2^*\gamma}(E_n)}.\end{aligned} \tag{5}$$

$C_{\rm nor}$ is the normalization factor defined by experimental conditions including the target thickness, the beam current, and the detector efficiency, etc. ϵ_2 and ϵ_1 can be canceled for charge particles because the two surrogate reactions are always measured with the same experimental setup. The normalization factor $C_{\rm nor}$ can be evaluated by correcting the target thickness, the beam current, and the gamma efficiency $\epsilon_{\gamma1}$, $\epsilon_{\gamma2}$ of the two surrogate reactions. After $N_{B1*\gamma}(E_n)$ and $N_{B2*\gamma}(E_n)$ obtained in experiment, the aimed reaction $\mathrm{A1}(n,\gamma)\mathrm{B1}$ cross section can be extracted with the known cross section of the reference reaction $\mathrm{A2}(n,\gamma)\mathrm{B2}$. Because the total number of the compound nucleus $N_{B^*}(E_{\rm ex})$ is not needed in SRM, uncertainties arising from $N_{B^*}(E_n)$ can be avoided.

In this work, the $^{91}\mathrm{Zr}(n,\gamma)^{92}\mathrm{Zr}$ and $^{93}\mathrm{Zr}(n,\gamma)^{94}\mathrm{Zr}$ reactions are chosen to check the surrogate ratio method. The compound nuclei $^{92}\mathrm{Zr}^*$ and $^{94}\mathrm{Zr}^*$ have a similar level structure, which is beneficial to make the CN formation cross-section ratio close to 1. Furthermore, the availability of directly measured neutron-induced data is crucial to check the validity of SRM via two-neutron transfer channels using $^{90}\mathrm{Zr}(^{18}\mathrm{O},^{16}\mathrm{O})$ and $^{92}\mathrm{Zr}(^{18}\mathrm{O},^{16}\mathrm{O})$ reactions. The γ rays emitted in deexcitation of compound nuclei $^{92}\mathrm{Zr}^*$ and $^{94}\mathrm{Zr}^*$ were detected in coincidence with outgoing $^{16}\mathrm{O}$ particles to obtain the ratio $N_{^{94}\mathrm{Zr}^*\gamma}(E_n)/N_{^{92}\mathrm{Zr}^*\gamma}(E_n)$. The indirectly determined $^{93}\mathrm{Zr}(n,\gamma)^{94}\mathrm{Zr}$ cross section with SRM is compared to the directly measured one.

III. EXPERIMENTS

The experiment was carried out at the Tandem accelerator of Japan Atomic Energy Agency (JAEA). A schematic layout of the experimental setup is shown in Fig. 1. An $^{18}\mathrm{O}$ beam with energy of 117 MeV was bombarded to the isotopically enriched zirconium target, which was made in the form of self-supporting metallic foil. The $^{90}\mathrm{Zr}$ target has a thickness of 300 μg/cm^2 and the isotopical enrichment was 99.4%, while the $^{92}\mathrm{Zr}$ target has a thickness of 315 μg/cm^2 and the isotopical enrichment was 94.6%. Downstream of the target, a silicon $\Delta E-E$ telescope was used to identify the light ejectile particles [32]. Two $\mathrm{LaBr_3(Ce)}$ detectors with a size of 4 inch in diameter $\times$5 inch in length were used for γ-ray detection [33]. A Faraday cup was installed to collect the $^{18}\mathrm{O}$

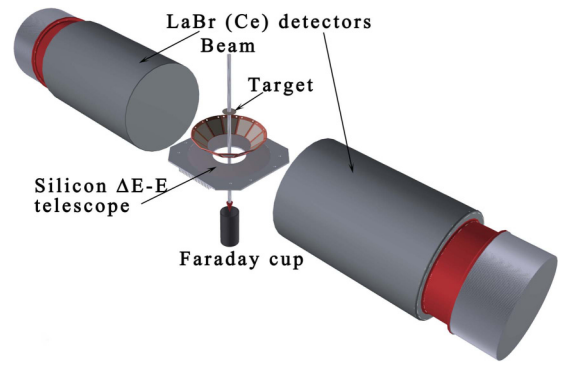

FIG. 1. Schematic layout of the experimental setup.

beam current for the purpose of normalization. The ^{18}O beam was kept to about 5 enA.

The ΔE detectors with trapezoidal shape are arranged to form a ring shape around the beam axis to collect efficiently the scattered ejectile particles in an angular range of 22°–39° relative to the beam direction. The thickness of the ΔE detector is 75 μm. The E detector is an annular-type detector and has 16 ring-shaped strips, by which the scattering angle of the ejectile can be defined with the angular resolution of around 1.2°. The thickness of the E detector is 300 μm. The two $LaBr_3$(Ce) γ detectors were placed perpendicular to the beam direction at a distance of about 150 mm from the target. The efficiency of the $LaBr_3$ detectors were determined with the ^{137}Cs and ^{60}Co standard γ sources; the absolute peak efficiency of each detector is about 0.45% at $E_\gamma = 1173.2$ keV.

Two reactions were measured in the same experimental setup. Irradiation time for each zirconium target was about 2 days, and the accumulated number of ejectile ^{16}O was roughly 1.1×10^6 and 1.2×10^6 for the ^{92}Zr and ^{90}Zr targets, respectively. The detected γ rays from ^{92}Zr* and ^{94}Zr* were about 1.9×10^3 and 1.2×10^3, respectively.

IV. DATA ANALYSIS

Figure 2 shows the two-dimensional plot of ejectile particles on the ΔE vs E_t, where E_t is the sum of energy loss in the ΔE detector and the residual energy in the E detector. The energy resolution for ^{16}O was about 1 MeV at full width at half maximum (FWHM). The ^{16}O, ^{17}O, ^{18}O, and ^{19}O are clearly distinguished.

A cut was set to select ^{16}O events which corresponds to the formation of ^{92}Zr* or ^{94}Zr* via (^{18}O,^{16}O) transfer reaction. The excitation energy E_x of ^{92}Zr* or ^{94}Zr* was deduced from the energy of ^{16}O by reconstructing the two-body kinematics on an event-by-event basis. To analyze the γ-ray spectra, an $E_x - E_\gamma$ two-dimensional matrix was formed. γ-ray spectra coming from the resonance region of ^{94}Zr* and ^{92}Zr* above the neutron threshold are shown in Fig. 3. Because ^{92}Zr and ^{94}Zr are both even-even nuclei, the de-excitation of their high-lying resonance states is expected to proceed overwhelmingly through the first 2^+ state to the 0^+ ground-state doorway transition. The energy of the transition is 919 keV for ^{94}Zr*, and 934 keV for ^{92}Zr*. Indeed, these are the most intense

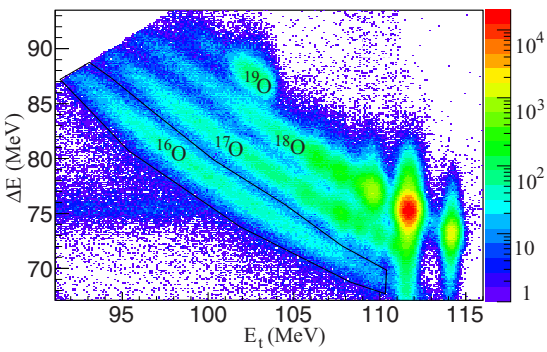

FIG. 2. Scatter plot of energy loss vs total energy of the reaction products from ^{18}O + ^{90}Zr.

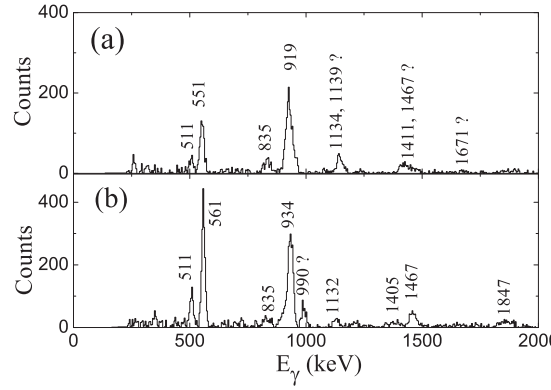

FIG. 3. γ-ray spectrum of CN ^{94}Zr*(a) and ^{92}Zr*(b), respectively. γ rays were detected by $LaBr_3$ detectors in coincidence with outgoing ^{16}O particles.

γ lines seen in Figs. 3(a) and 3(b), respectively. For ^{94}Zr* as shown in Fig. 3(a), the 551-keV $4_1^+ \rightarrow 2_1^+$ and 1139-keV $3_1^- \rightarrow 2_1^+$ transitions are also observed, which correspond to the 561- and 1405-keV γ lines for ^{92}Zr* seen in Fig. 3(b). A small amount of 1847-keV γ rays corresponding to the $2_2^+ \rightarrow 0_{g.s.}^+$ γ transition is observed in ^{92}Zr*. The 1467-keV γ line is from the self-background of $LaBr_3$ detectors, because of the long-lived ^{138}La. A γ line with an energy of about 835 keV is seen in both spectra; it is the Doppler-shifted 871-keV γ ray from the ^{17}O de-excitation, which indicates a fraction of ^{17}O mixing in the ^{16}O cut. Although the ^{17}O mixing may bring uncertainties to the counting of ^{16}O, the exact number of ^{16}O is no longer needed in SRM£¬and the yield does not influence the results obtained in the SRM.

Next, we focused on the absolute intensity of the 919- and 934-keV γ lines. The absolute branching ratio of 919- and 934-keV γ lines of ^{94}Zr and ^{92}Zr was taken as 94.9% and 97.2%, respectively; these are from the evaluated data [34] of ^{94}Y $\rightarrow$ ^{94}Zr and ^{92}Y $\rightarrow$ ^{92}Zr β decays. The net areas of these two γ lines were deduced in a bin width of $E_n = 1000$ keV; $N_{^{94}Zr^*\gamma}(E_n)$ and $N_{^{92}Zr^*\gamma}(E_n)$ were then obtained. After the correction of the integrated ^{18}O beam current, the target thickness, the absolute detection efficiency of the $LaBr_3$ detectors, and the absolute branching ratio of γ lines, the normalization factor C_{nor} was determined. The γ-decay probability ratio was finally obtained, as shown in Fig. 4. The energy resolution in the equivalent neutron energy E_n is about 1 MeV; eight data points were deduced within $E_n = 0$–8 MeV accordingly.

V. RESULTS

Because the level structures of ^{92}Zr and ^{94}Zr are similar, the excitation functions of ^{91}Zr$(n,\gamma)^{92}$Zr and ^{93}Zr$(n,\gamma)^{94}$Zr calculated by Hauser-Feshbach theory have the same behavior at $E_n < 1$ MeV. The difference of the two (n,γ) cross sections can be approximated by a constant at this energy range. The directly measured cross sections of the ^{91}Zr$(n,\gamma)^{92}$Zr [35] and ^{93}Zr$(n,\gamma)^{94}$Zr [36] reactions at $E_n < 1$ MeV are both available; we can check the SRM by comparing the deduced ^{93}Zr$(n,\gamma)^{94}$Zr cross sections to the directly measured

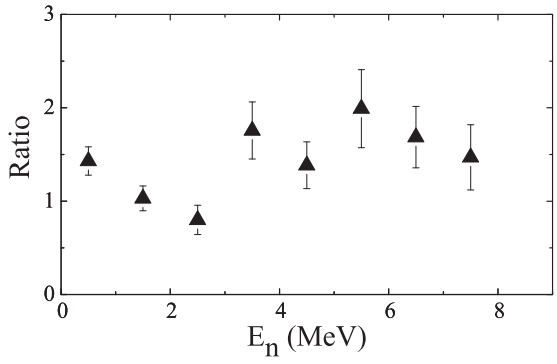

FIG. 4. The γ-decay probability ratio of compound nuclei ^{94}Zr* and ^{92}Zr*.

ones. ^{93}Zr$(n,\gamma)^{94}$Zr reaction cross sections were determined by the average ratio of 1.43 ± 0.15 multiplying the known ^{91}Zr$(n,\gamma)^{92}$Zr cross sections [35]. The deduced ^{93}Zr$(n,\gamma)^{94}$Zr reaction cross sections are compared in Fig. 5 with the directly measured ones, and one can see that they are in reasonable agreement.

Furthermore, according to the works of Chiba and Iwamoto [23], the γ-decay probability ratio is relatively insensitive to the spin-parity distribution of CN at neutron energies $E_n >$ 3 MeV; the (n,γ) cross sections deduced by the SRM in the high energy region are thought to be closer to the directly measured data. Because there are no experimental data at the neutron energies larger than 1 MeV, the ENDF/B-VII.1 cross section of the ^{91}Zr$(n,\gamma)^{92}$Zr reaction is used. The deduced ^{93}Zr$(n,\gamma)^{94}$Zr cross sections are shown in Fig. 6. One can see that the deduced ^{93}Zr$(n,\gamma)^{94}$Zr reaction cross sections agree well with ENDF/B-VII.1 data at $E_n > 3$ MeV.

VI. DISCUSSION AND CONCLUSION

With the parameters constrained by the deduced cross section of the ^{93}Zr$(n,\gamma)^{94}$Zr reaction at $E_n > 3$ MeV, a UNF code [37,38] can be used to calculate the cross section in the low energy region. The results are shown in Fig. 7 in comparison with the extracted data by SRM and directly

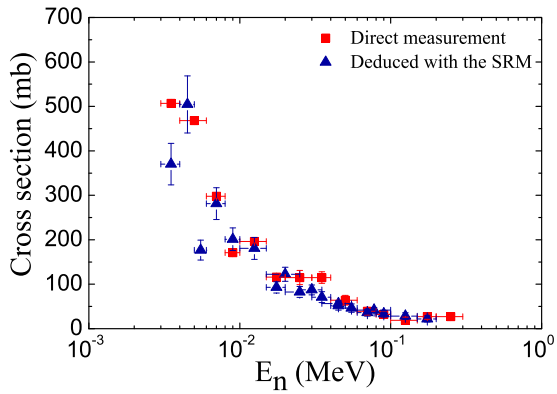

FIG. 5. Cross section of ^{93}Zr$(n,\gamma)^{94}$Zr in low energy region. The red squares are directly measured data [36]; the blue triangles are deduced by the γ-decay probability ratio and ^{91}Zr$(n,\gamma)^{92}$Zr cross sections [35].

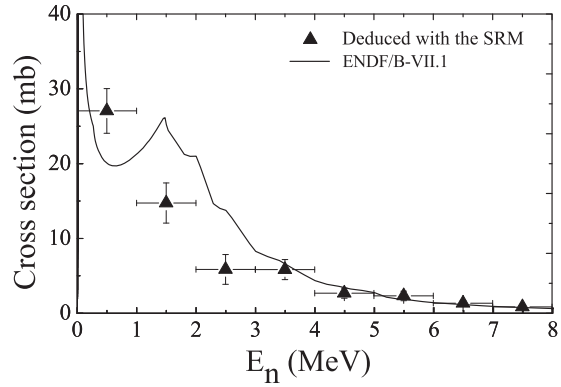

FIG. 6. Cross section of ^{93}Zr$(n,\gamma)^{94}$Zr. The triangles are deduced by the measured γ-decay probability ratios and ^{91}Zr$(n,\gamma)^{92}$Zr ENDF/B-VII.1 cross sections. The solid curve is the ENDF/B-VII.1 data of ^{93}Zr$(n,\gamma)^{94}$Zr.

measured cross sections for the ^{93}Zr$(n,\gamma)^{94}$Zr reaction. The calculated cross sections agree well with the directly measured ones in the low neutron energy region.

In summary, two-neutron transfer reactions (^{18}O ,^{16}O) were employed to check the SRM for the determination of the (n,γ) reaction cross section. The ^{93}Zr$(n,\gamma)^{94}$Zr reaction cross sections are determined in a wide energy region of 0–8 MeV using the reference cross sections of the ^{91}Zr$(n,\gamma)^{92}$Zr reaction and the measured γ-decay probability ratios. The deduced ^{93}Zr$(n,\gamma)^{94}$Zr reaction cross sections are found lower than the ENDF/B-VII.1 data at $E_n = 1$–3 MeV, but at $E_n < 1$ MeV and $E_n > 3$ MeV the deduced cross section agree well with directly measured one and ENDF/B-VII.1 data, respectively. Although the absolute surrogate method may suffer from the spin-parity sensitivity problem at low neutron energy region, the present data imply that the sensitivity of γ-decay probability ratio to the CN spin-parity distribution is partially reduced in SRM. Furthermore, the SRM data can be used to provide a restriction of the model parameters in theoretical calculation at the relatively high neutron energy region, which in turn gives a reasonable estimation of the (n,γ) cross sections in the low energy region.

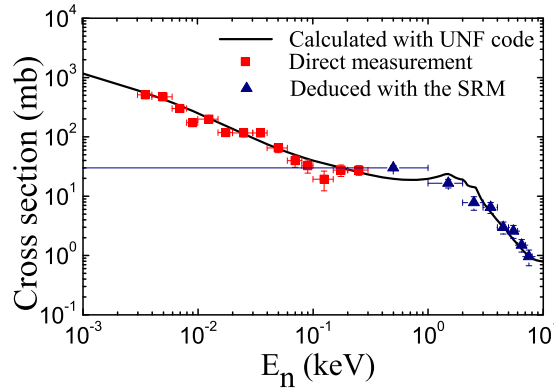

FIG. 7. Cross section of ^{93}Zr$(n,\gamma)^{94}$Zr. The blue triangles are deduced by the γ-decay probability ratios and ^{91}Zr$(n,\gamma)^{92}$Zr ENDF/B-VII.1 cross section; the red squares are directly measured data [36] and the solid curve is the result calculated by UNF code [37].

ACKNOWLEDGMENTS

We thank JAEA Tandem accelerator facility staff for their help in the experiment. This work was supported by the National Natural Science Foundation of China under Grants No. 11375269, No. 11490560, No. 11321064, and No. 11205247, and the National Basic Research 973 Program of China under Grant No. 2013CB834406.

[1] F. Käppeler *et al.*, Rep. Prog. Phys. **52**, 945 (1989).
[2] O. Straniero *et al.*, Nucl. Phys. A **777**, 311 (2006).
[3] L.-S. The *et al.*, Astrophys. J. **655**, 1058 (2007).
[4] F. Käppeler *et al.*, Rev. Mod. Phys. **83**, 157 (2011).
[5] M. Lugaro *et al.*, Astrophys. J. **780**, 95 (2014).
[6] W. Younes and H. C. Britt, Phys. Rev. C **67**, 024610 (2003).
[7] W. Younes and H. C. Britt, Phys. Rev. C **68**, 034610 (2003).
[8] M. Petit *et al.*, Nucl. Phys. A **735**, 345 (2004).
[9] S. Boyer *et al.*, Nucl. Phys. A **775**, 175 (2006).
[10] G. Kessedjian *et al.*, Phys. Lett. B **692**, 297 (2010).
[11] J. D. Cramer and H. C. Britt, Nucl. Sci. Eng. **41**, 177 (1970).
[12] V. F. Weisskopf and D. H. Ewing, Phys. Rev. **57**, 472 (1940).
[13] C. Plettner *et al.*, Phys. Rev. C **71**, 051602(R) (2005).
[14] J. T. Burke *et al.*, Phys. Rev. C **73**, 054604 (2006).
[15] B. F. Lyles *et al.*, Phys. Rev. C **76**, 014606 (2007).
[16] B. K. Nayak *et al.*, Phys. Rev. C **78**, 061602 (2008).
[17] S. R. Lesher *et al.*, Phys. Rev. C **79**, 044609 (2009).
[18] B. L. Goldblum *et al.*, Phys. Rev. C **80**, 044610 (2009).
[19] J. J. Ressler *et al.*, Phys. Rev. C **83**, 054610 (2011).
[20] J. E. Escher *et al.*, Rev. Mod. Phys. **84**, 353 (2012).
[21] C. Forssen *et al.*, Phys. Rev. C **75**, 055807 (2007).
[22] J. E. Escher and F. S. Dietrich, Phys. Rev. C **81**, 024612 (2010).
[23] S. Chiba and O. Iwamoto, Phys. Rev. C **81**, 044604 (2010).
[24] B. L. Goldblum *et al.*, Phys. Rev. C **85**, 054616 (2012).
[25] N. D. Scielzo *et al.*, Phys. Rev. C **81**, 034608 (2010).
[26] G. Boutoux *et al.*, Phys. Lett. B **712**, 319 (2012).
[27] B. L. Goldblum, S. G. Prussin, U. Agvaanluvsan, L. A. Bernstein, D. L. Bleuel, W. Younes, and M. Guttormsen, Phys. Rev. C **78**, 064606 (2008).
[28] B. L. Goldblum, S. G. Prussin, L. A. Bernstein, W. Younes, M. Guttormsen, and H. T. Nyhus, Phys. Rev. C **81**, 054606 (2010).
[29] J. M. Allmond *et al.*, Phys. Rev. C **79**, 054610 (2009).
[30] R. Hatarik *et al.*, Phys. Rev. C **81**, 011602(R) (2010).
[31] J. E. Escher and F. S. Dietrich, Phys. Rev. C **74**, 054601 (2006).
[32] K. Nishio *et al.*, Phys. Procedia **64**, 140 (2015).
[33] H. Makii *et al.*, Nucl. Instrum. Methods Phys. Res., Sect. A **83**, 797 (2015).
[34] R. B. Firestone *et al.*, *Table of Isotopes*, Version 1.0 (John Wiley and Sons, New York, 1996).
[35] A. R. d. L. Musgrove *et al.*, Aust. J. Phys. **30**, 391 (1977).
[36] R. L. Macklin, Astrophy. Spa. Sci. **115**, 71 (1985).
[37] J. S. Zhang, Nucl. Sci. Eng. **114**, 55 (1993).
[38] J. S. Zhang, Nucl. Sci. Eng. **142**, 207 (2002).